Available online at www.sciencedirect.com
SCIENCE DIRECT®
Chemical Physics xxx (2003) xxx–xxx
Chemical Physics
www.elsevier.com/locate/chemphys

Hydration water dynamics of a completely hydrophobic oligopeptide

Daniela Russo[a,*,1], Piero Baglioni[a], Elisa Peroni[a], Jose' Teixeira[b,2]

[a] Department of Chemistry, University of Florence, Via della Lastruccia 3, 50119 Sesto Fiorentino, Firenze, Italy
[b] Laboratoire Léon Brillouin (CEA/CNRS), Saclay CEA, 91191 Gif-sur Yvette Cedex, France

Received 31 October 2002; in final form 4 March 2003

Abstract

The dynamics of hydration water of a completely deuterated penta-alanine peptide has been studied by incoherent quasi-elastic neutron scattering. Measurements have been made at different hydration levels (7%, 30%, 50%, 90%), and on the dried powder (0%) which contains one structural water molecule. The dynamical contribution of this first hydration molecule of water is characteristic of a slow rotational motion with a relaxation time, τ_1, of 2.2 ps, similar to what is found in supercooled water dynamics. Adding two more hydration water molecules (7%) the rotational motion of the first water is coupled with the new diffusive motion and the dynamics profile can be, in first approximation, described through a rotational jump model. The results suggest a behavior similar to that of bulk water at 2 °C. At higher levels of hydration, the mobility of new molecules of water approaches that of bulk water, with a rotation relaxation time of 1 ps and a confined diffusing motion. However the residence time value, τ_0, is of the same order of magnitude as supercooled water at $T = -10$ °C.

1. Introduction

Proteins and nucleic acids must maintain specific three-dimensional structures to fulfill their functions. Interactions between water and these macromolecules largely contribute to their structural stability in aqueous solutions [1,2]. The first hydration shell of proteins has a 10–20% density increase as compared to bulk water [3]. This is a result of the combination of polar and apolar groups on the surface of proteins, which preferentially order the surface waters. The polar groups are able to create a structured hydration shells through ionic and hydrogen bonding interactions. Apolar groups promote cluster formation. The different interactions between hydrophilic and hydrophobic aminoacids and molecules of water has been studied using Raman spectroscopy, which probed the change in the OH stretch of water that

* Corresponding author. Tel.: +1-15-10-486-5077; fax: +1-15-10-486-5077.
E-mail addresses: drusso@lbl.gov (D. Russo), teix@llb.saclay.cea.fr (J. Teixeira).
[1] Present address: Bioengineering Department, University of California, Berkeley, CA 94720, USA.
[2] Also corresponding author. Tel.: +33-1-69-08-66-50; fax: +33-1-69-08-82-61

0301-0104/03/$ - see front matter
doi:10.1016/S0301-0104(03)00200-3

is a function of amino acid hydrophobicity [4]. The number of water–water hydrogen bonds decreases in the following order apolar > polar > charged residue [4–6]. The side chain effects on the structure of water become more pronounced as the surface of the residue accessible to the solvent increases [4]. Also, infrared spectroscopy studies show that the size of water clusters around the side chain of hydrophobic amino acid increases in the following order Gly < Ala < Val < Ile, Leu [7].

The degree of plasticity of the protein, determined by the hydration levels, influences the internal motions [8,9]. Moreover, water plays an important role in the dynamics of biological macromolecules [10]. Unfortunately, experimental studies of this subject have been relatively rare and not systematic. The main problem is that water–monomer interactions fluctuate on a short time scale and involve many complex factors such as hydrogen bonds or hydrophobic interactions and different situations of water confinement. One of the principal limitations of these studies is that the most important techniques able to investigate the water dynamics give average information over all different kinds of interactions. Thus, it is impossible to distinguish the contribution arising from a hydrophobic and hydrophilic sites or between regions more or less exposed to the solvent [11,12]. Another real limitation has to do with the molecular environment. Being more interesting to study the molecules under physiological conditions, it is necessary to work with concentrated solutions (100–200 mg/ml). However, these concentration levels are difficult to attain in vitro due to aggregation and precipitation. On the other hand, at low concentrations of proteins, the contribution of bulk water is dominant and overwhelms the interesting effects of hydration water. To date there have been many important studies on hydrated powders [13–17].

In order to study more precisely the role of water as a function of its location, in a situation better defined than with a natural biological molecule, a completely homogeneous system has been studied. To investigate the hydrophobic effect on the dynamics of hydration water on a pico-second time scale we made use of incoherent quasi-elastic neutron scattering arising from protons of hydrated powder of a completely deuterated oligopeptide, penta-alanine. Alanine is the simplest hydrophobic amino acid, with a high natural propensity to form and stabilize helical structures [18–22]. The solid state conformation of poly-alanine has been well established by NMR experiment [23]. Results describe as a completely beta sheet conformation the structure of the tetra-alanine peptide; as a 92% beta sheet and 8% alpha helix the structure for alanine peptides up to 200 units; and as a structure with 85% of alpha helix and 15% of beta sheet for the poly-alanine with 333 units.

2. Materials and methods

2.1. Sample preparation

The penta-alanine peptides have been synthesized, in continuous flow, by solid phase using the Fmoc protection strategy. The Fmoc (9-fluoreilmetossicarbonile) group is used to protect the sensitive-amino group from deleterious reactions during the formation of a new peptide bond between the unprotected carboxyl group of the free amino acid and the unprotected-amino group of the growing peptide chain. It is labile in basic environment (20% of piperidin + dimethylformamide). In this technique, the C-terminal amino acid is first attached to an insoluble polymer support; the peptide is built up stepwise, amino acid by amino acid towards the N-terminus. At the end of the reaction, the peptide is removed from the resin and all the chain protection groups are simultaneously cleaved with 95% trifluoroacetic acid/water (TFA). This cleavage provides a free acid peptide form. The peptide is provided of the CF_3COO^- counterion. The poly-crystalline form has a total charge equal to zero.

The resin is a polystyrene matrix (Tenta Gel S PBH, RAPP Polymer, Germany), with an affinity of 0.26 mmol/g. The completely deuterated Fmoc–Ala–OH amino acids were purchased from CDN Isotopes, Canada.

For the preparation of the sample, at different hydration levels (h), we adopted the following procedure. The solid state penta-alanine peptides

have been exposed to an atmosphere at 100% of humidity, for *a period* of time. As a function of exposed time, we could determine the various hydration degrees, simply by weight difference between the same sample before (dry) and after the exposition (hydrated). We do want focus the attention that all the hydration values are calculated relatively to the dry sample (0%), which contains one structural water molecule. Each hydrated sample, has been dissolved in H_2O, lyophilized and hydrated before to be used for the following runs.

The neutron measurements were performed at the following hydration levels: 7%, 30%, 50% and 90%.

In Table 1 is reported the number of the added water molecules for each h level, the total number of molecules of water for each h level and the water relative contribution to the total incoherent scattering.

2.2. Experimental procedure

The experiment was carried out at the Orphée reactor of the Léon Brillouin Laboratory, using the MIBEMOL time of flight spectrometer. The spectrometer was operated with an incident energy of 1.28 meV, a wavevector range of $0.5 < Q < 1.5$ A^{-1}, and an energy resolution HWHM (half width at half maximum) of 0.018 meV. All samples were placed in a slab 1 mm tick, oriented 45.8° with respect to the incident beam. All samples were measured for 24 h at each hydration. All experimental spectra were corrected for the contribution due to the sample holder. They were also normalized using the vanadium standard and corrected for the transmission and geometry effects. The resulting data were analyzed with the LLB programs.

Table 1
Number of molecules of water as a function of the hydration level

Hydration h (%)	No. of added molecule of water/ peptide	No. of total molecules of water/ peptide	% of total incoherent scattering
0	**0.84**	**0.84**	20
7	1.96	2.8	45
30	8.4	9.24	72
50	14	14.84	80
90	25	25.84	94

2.3. Data analysis

The analysis of molecular dynamics by quasi-elastic neutron scattering is based on the very large incoherent cross-section of the proton. For any sample containing hydrogen atoms, essentially all the scattered intensity is due to them. In QENS experiments one analyses small energy changes within a window defined by the energy of the incident neutron beam and the characteristics of the spectrometer. Isotopic substitution is often used to reduce the contribution of some hydrogen atoms. For example, in our study, we synthesized deuterated samples of penta-alanine in order to reduce the otherwise dominant contribution of the hydrogen atoms of the alanine.

The central line of a QENS spectrum contains a priori two main contributions. One purely elastic is due to immobile hydrogen atoms, the other, quasi-elastic is due to different classic motions and corresponds to the Fourier transform of the correlation function $\langle \mathbf{r}_H(0) \cdot \mathbf{r}_H(t) \rangle$, where $\mathbf{r}_H(t)$ represents the position of each atom at time t and $\langle \cdots \rangle$ represents an ensemble average over all the atoms. The elastic component, which is theoretically a Dirac function at $\omega = 0$, is in practice broadened by the instrumental resolution which establishes a limit to the observation of the slowest motions. More precisely, the "elastic" component contains the contribution due to slow motions superimposed on that of immobile hydrogen atoms.

The analysis of the quasi-elastic component can be made in the framework of different models. For our samples, the high density imposes a restricted molecular diffusion that superimposes on the internal motions of the molecule. The last do not depend on Q, a property which allows an analytical separation from molecular diffusion. At times long enough, the molecular diffusion is described by Fick's law: the quasi-elastic line is a Lorentzian with a HWHM $\Gamma = DQ^2$, where D represents the molecular self-diffusion.

At short distances, i.e., at large values of Q, the molecule may be seen inside the cage formed by its neighbors. This localization in a small volume

corresponds to a constant value of Γ, from which one may extract a "residence time" by $\tau_0 = 1/\Gamma(Q \to \infty)$. This simplified approach of diffusion at short times, called jump model, does not apply necessarily but it is often a reasonable interpretation of the saturation of Γ at large values of Q.

The internal motions of the molecule may be described by a model of rotation, which describes the motion of the hydrogen atom inside a small volume. The simplest situation corresponds to the random motion on the surface of a sphere of radius a. In this case, the amplitude of the scattered intensity is a sum of Lorentzians weighted by spherical Bessel functions. More important and more general, the first component is elastic (because it represents the finite volume accessible to the atomic motions). It is called "Elastic incoherent structure factor (EISF)". It corresponds to the form factor of the restricted volume and is an exceptional case where incoherent scattering contains structural information.

In what follows, the plausibility of the application of these models to our samples is discussed in detail.

3. Results and discussion

3.1. Peptide structure characterization

The penta-alanine peptide presents in the solid state form a beta sheet conformation [23]. IR spectroscopy has been used to monitor change in % beta sheet content upon hydration. The hydrogenated sample, diluted with KBr salt (to avoid signal saturation), has been hydrated with deuterated water at 0%, 35%, 52%, 66%, 80%. Each spectra has been measured between 4000 and 1000 cm^{-1}. Any significant variations have been detected in the amide I (stretch of C=O) and amide II (N–H deformation) region (data not show). It has been assumed that the secondary structure is not changing upon hydration.

Measuring the heat capacity variation, between 20 and 120 °C, the existence of strongly bonded water to the peptide has been detected. This structural water is present in a quantity equal to one molecule of water for each molecule of penta-alanine.

3.2. Hydration water dynamics

The incoherent peptide cross-section versus the incoherent water cross-section is represented in Table 2. From these values, the total incoherent peptide cross-section has been calculated to be equal to 524.72 barns, three times the contribution of a single molecule of water.

As described in the previous section, the penta-alanine peptide in solid state assumes a beta sheet configuration. As in the case of completely beta sheet proteins [24], the labile protons of the peptide, which belong to the backbone and are involved in very stable hydrogen bond, do not have, at room temperature, a quasi-elastic dynamics in the pico-second time scale. In addition the incoherent quasi-elastic CD_3 methyl contribution (30.75 barns) is negligible with respect to one molecule of water contribution (160.4 barns). Therefore, assuming that the elastic line is, mostly, arising from the peptide scattering, and the quasi-elastic from the water scattering, we expect that these contributions are equivalent when the number of hydration molecules of water equals three. In other words, we expect that the quasi-elastic contribution is equal or greater than the elastic scattering, respectively, for a number of hydration waters molecules equal or greater than three. In order to experimentally prove this and also to demonstrate that the quasi-elastic incoherent scattering is strictly related to the hydration water dynamics, a preliminary analysis, performed fitting

Table 2

Atoms	N	Atom $X_{s\ inc}$	Tot. $X_{s\ inc}$
Peptide incoherent cross-section			
C	17	0.001	0.017
N	5	0.5	2.5
O	8	0.0008	0.0064
D	20	2.05	41
F	3	0.0008	0.0024
H	6	80.2	480
Water incoherent cross-section			
H_2	160.4		
O	0.0008		

all the data with elastic and one quasi-elastic contribution, has been done. Fig. 1 shows the elastic and the quasi-elastic intensity as a function of the number of hydration molecules of water, at various values of Q. It appears that the elastic line does not have any dependence on Q and on the hydration; instead the quasi-elastic line presents dependence on both parameters. It is very important to remark also that the elastic and quasi-elastic intensity cross each other, for each Q value, when the number of molecules of hydration water equals three, as predicted from the previous calculation of the total incoherent cross-section. The total agreement of the experimental value of the crossover with the calculated one confirms the high fidelity of the sample preparation and also of the presented neutron data.

This preliminary analysis has been crucial to unambiguously define how to subtract the peptide contribution in the following water dynamics data analysis.

3.3. Dry peptide

The spectra analysis has been performed using a superposition of one elastic and one quasi-elastic line. Supported by the previous results, we assume that the quasi-elastic component arises exclusively from the structural water dynamics.

Fig. 2 shows the experimental variation of the half width at half maximum, $\Gamma(Q)$, with Q. The HWHM of the Lorentzian function is constant in Q, with an average value of 0.1 meV, what suggests the presence of a confined motion, like a diffusion in a sphere with a radius $a_{\mathrm{diff}} < 2$ Å ($T = $ const. up to $Q = \pi/a$) [23], or a pure rotational motion.

To characterize this confined motion, the variation of the amplitude $A(Q)$, against Q, of the Lorentzian function has been analyzed.

If the contribution described from the quasi-elastic component arises from the rotation of the protons confined in a sphere around the oxygen, the amplitude A(Q) follows:

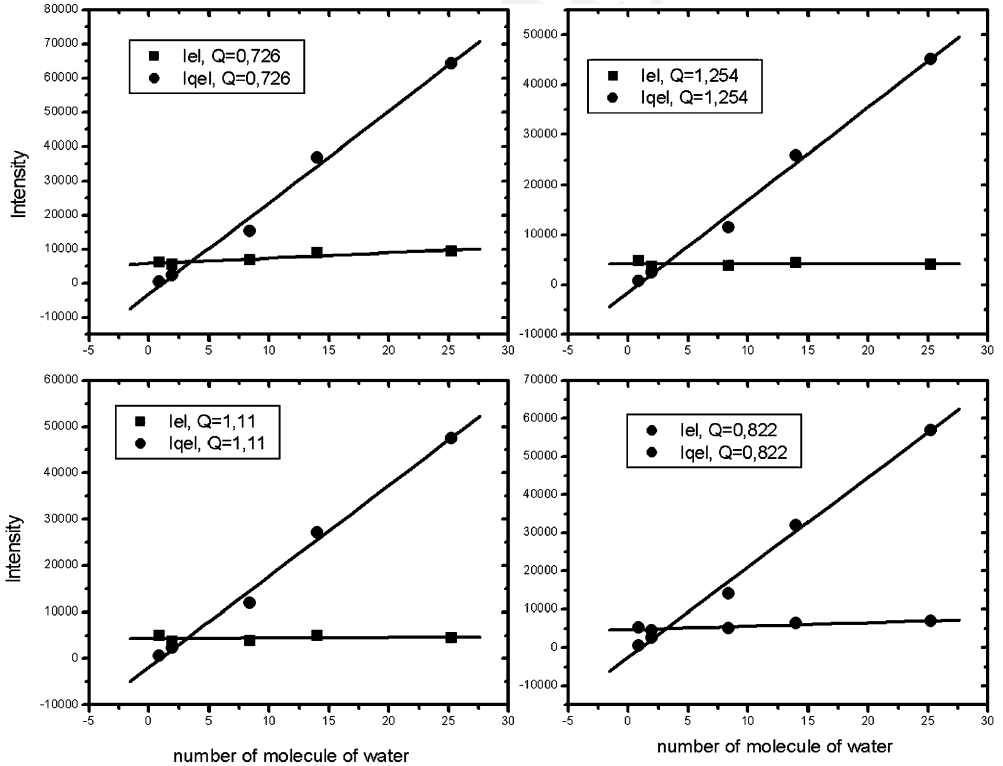

Fig. 1. Elastic and quasi-elastic intensities of deuterated penta-alanine, as a function of the number of water molecules, for the elastic momentum transfers $Q = 0.726$, 1.254, 1.11 and 0.822 A^{-1}.

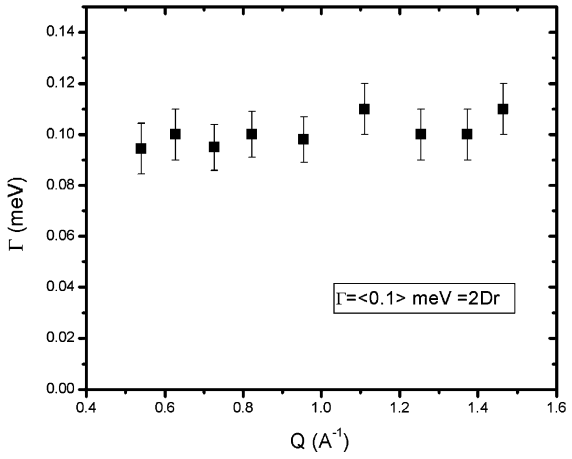

Fig. 2. Half width at half maximum, $\Gamma(Q)$, of the Lorentzian component, as a function of Q, for the peptide at the hydration level $h = 0$.

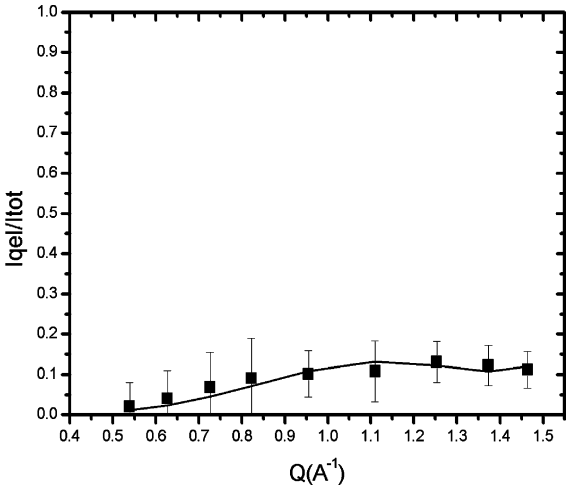

Fig. 3. Q dependence of the relative experimental quasi-elastic intensity, for the peptide at the hydration level $h = 0$. The solid line is the fit based on Eq. (1), with a number of families of spheres equal to two.

$$A(Q) = 3j_1^2(Qa_{\mathrm{rot}}) = 3 \times \left[\frac{\sin(Qa_{\mathrm{rot}}) - (Qa_{\mathrm{rot}})\cos(Qa_{\mathrm{rot}})}{(Qa_{\mathrm{rot}})^2}\right]^2 \quad (1)$$

where a_{rot} is the radius of the sphere where the rotation occurs and $j_1(Qa_{\mathrm{rot}})$ is the first order spherical Bessel function. The corresponding relaxation time, which characterizes the lifetime of the first hydrogen bond, is $t_1 = 2$ ps. In the fitting procedure, it has been taken into account a prefactor factor x, which is a measure of the fraction of water contribution to the total scattering.

The data adjustment to the Eq. (1) has been performed using, a distribution of spheres, with a number of families of spheres equal to two. The value of the parameter x has been measured to be equal to 17%, which is in completely accord to that one estimated in Table 1. In addition, the 97.5% of this contribution arises from rotational motion characterized from a sphere of radius $a_{\mathrm{rot}} = 0.6$ Å and the 2.5% from rotational motion with $a_{\mathrm{rot}} = 2.8$ Å. The second set of parameters has been considered like a correction term for the model (Eq. (1)). Fig. 3 shows the fitting procedure using Eq. (1) with a distribution of spheres.

In the case that the monitored motion is a very confined diffusion, in a sphere of radius a_{diff}, the amplitude of the Lorentzian function has to follow the term A_{01} of Volino and Dianoux model [25]. The parameters inferred from this adjustment, $a_{\mathrm{diff}} = 2.56$ Å and $x = 0.004$, do not correspond to the attended value ($a_{\mathrm{diff}} < 2$ Å, $x = 0.2$).

From the analysis of the amplitude of the quasi-elastic component, it has been assumed that the first molecule of hydration water is characteristic of a rotational motion. The structural protons, strongly bonded to the peptide, can only rotate without diffusing.

The peptide elastic contribution has been determined, taking into account this first important conclusion.

Fig. 4 shows the dependence on Q of the experimental elastic intensity fraction; in addition is also shown the EISF arising from the water protons and the peptide constant contribution. The total elastic component is equal to $Iel = A + x * j_0(Qa_{\mathrm{rot}})^2$, where the first term is arising from the peptide scattering and the second one from the protons. $j_0(Qa_{\mathrm{rot}})$ is the Bessel function of order zero, it describes the hydration water EISF. Using the previous defined values of x and a, it has been possible to determine the elastic contribution of the peptide. As expected, this contribution is constant on Q, and is the dominant part of the

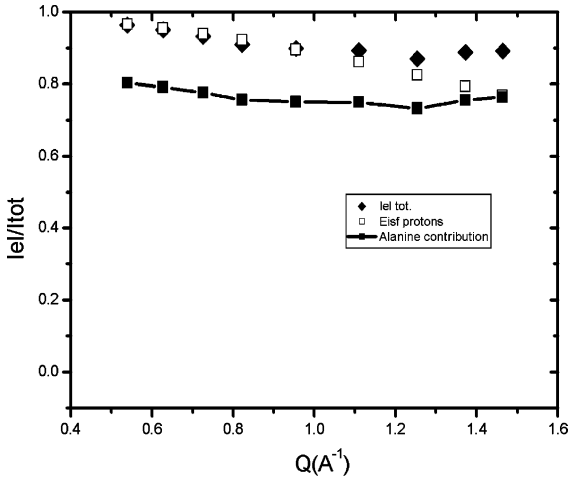

Fig. 4. Q dependence of the relative experimental elastic intensity for the dry peptide. The calculated structural water contribution and the extrapolated peptide contribution are also represented.

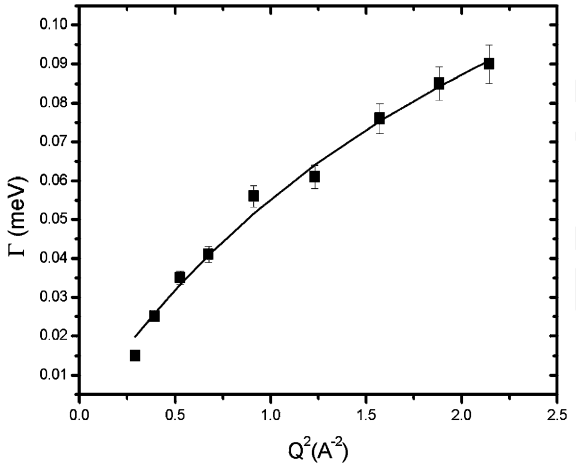

Fig. 5. Half width at half maximum, $\Gamma(Q)$, plotted versus Q^2, for the peptide at $h = 0.07$. The solid line is the fit based on the random jump model.

elastic scattering. Being this contribution constant with the hydration, the inferred value has been then used on the following data analysis, to take into account of the penta-alanine contribution.

3.4. Peptide hydrated at 7%

The analysis of the spectra has been performed using an elastic and one quasi-elastic line. Fig. 5 shows the dependence on Q^2 of the half width at half maximum of the Lorentzian function. The different dependence on Q from the dry peptide, suggests the presence of a new diffusive motion. In addition, it is difficult to separate the dynamics of the first water (slow rotation) from the dynamics of the two new added waters because there is a coupled dynamics. Supported by the absence of a plateau at small Q value (which excludes local diffusion), we propose, in first approximation, that diffusion for random rotational jump or continuous diffusion perturbed from rotational motion could be a valid model to describe the dynamics of hydration water of the peptide hydrated at 7%.

The dynamics profile has been, in first approximation, described through a rotational jump model. The defined dynamics parameters have been: the residence time τ_0, which corresponds to the time necessary to break a hydrogen bond and allows jump diffusion; and the diffusion coefficient D. The inferred residential time is equal to $\tau_0 = 2.56$ ps and the diffusion coefficient equal to $D = 1.05 \times 10^{-5}$ cm^2/s.

The lack of a defined plateau at high Q value means that the residence time value is affected by a relatively big error, and a measurement with a different configuration would be necessary.

From the experimental elastic intensity and from the previous analysis the hydration water EISF has been determined. Taking into account the rotational elastic contribution of the first hydration water and the presence of a coupled dynamics, the hydration water EISF can be written as: $\mathrm{EISF} = \mathrm{EISF}(0) * \mathrm{EISF}_{\mathrm{newH_2O}}$. The first term, EISF(0), is arising from the slow rotation of the first molecule of water. The second term, $\mathrm{EISF}_{\mathrm{newH_2O}}$, take in account the contribution of the two new protons. The best fit to the EISF has been obtained by treating the second term like a rotation occurring in a sphere of radius $a_{\mathrm{rot}} = 0.5$ A, with a relative proton fraction equal to 0.4.

3.5. Peptide hydrated at 30%, 50% and 90%

The diffusion spectra have been analyzed for all the hydration levels using an elastic and two quasi-elastic lines. The quasi-elastic component has been well described from a large, L_2, (rotational con-

tribution) and a narrow, L_1, (translational) Lorentzian functions. These two components have been considered as two independent terms, and it has been assumed that the cross term, $L_2 * L_1$, is overwhelmed in the Lorentzian function L_2.

Fig. 6(a) shows the dependence on Q of Γ_2 (large Lorentzian) for all the different hydration levels. Fig. 6(b) shows the variation of Γ_1 versus Q^2 for the peptide hydrated up to 90% and for the free water diffusion ($D = 2.1 \times 10^{-5}$ cm^2/s).

The dynamical parameter Γ_2 is constant both on Q and on hydration level, with an average value of 0.24 meV. Taking advantage of the analysis of the dry peptide, we assume that this component arises from a rotational motion with a characteristic time of 0.9 ps. This result suggests the presence of large amplitude movement. This value is of the same order of magnitude as the hydrogen bond lifetime in bulk water [26,27]. At high hydration levels the slow rotation of the first bonded water, is buried into the signal of the new molecules of water, slowly approaching a behavior similar to that of bulk water. In fact, at low hydration levels, the molecules of water are isolated and able to form bonds only with the peptide; at the highest hydration levels the probability to forming hydrogen bonding with other water molecules is dominant.

The width of the narrow Lorentzian has been analyzed, in first approximation, with a jump model. The diffusion coefficient D, and the residence time τ_0 are listed for the three hydration levels on Table 3. The value of the diffusion coefficient, as a function of the number of molecules of water, slowly approaches the value of the diffusion coefficient in bulk water, while the characteristic residence time is almost independent of the hydration level. This aspect could be explained by the complete homogeneity of the sample and eventually also by the lack of structural cavities, which instead are present in proteins. It is plausible that, as long as the number of molecules of hydration

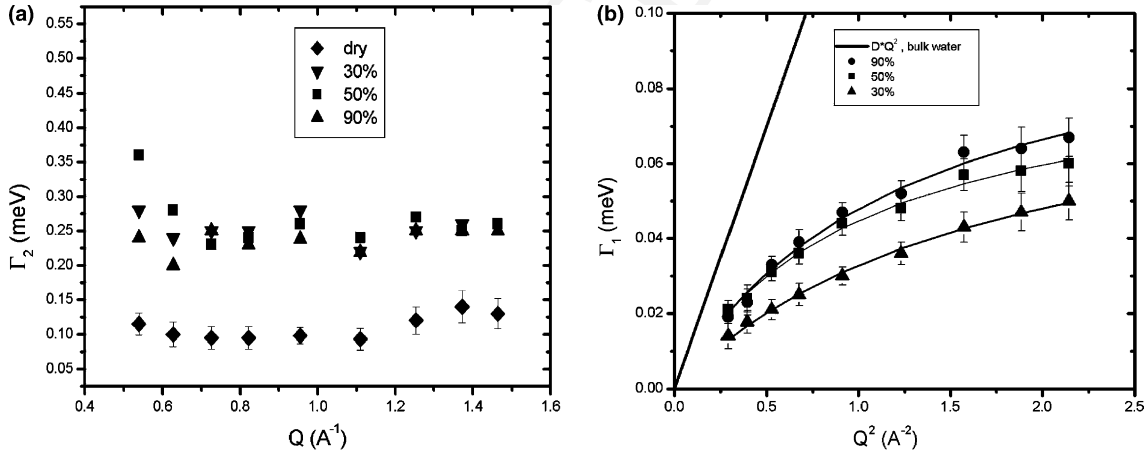

Fig. 6. (a) HWHM, $\Gamma_2(Q)$, of the Lorentzian function plotted versus Q corresponding to the rotational motions of protons, at different hydration levels. (b) HWHM, $\Gamma_1(Q^2)$, of the Lorentzian function plotted versus Q^2 corresponding to the translational motions of protons, at different hydration levels. The solid line represents bulk water self-diffusion.

Table 3
Diffusion coefficient, residence time and jump length evaluated from the high hydration level analysis

Hydration (%)	D (10^{-6} cm^2/s)	τ_0 (ps)	Jump length (Å)
90	13.61 ± 0.8	6.1 ± 0.3	1.47 ± 0.1
50	13.088 ± 0.6	7.4 ± 0.3	1.63 ± 0.1
30	7.75 ± 0.27	7.37 ± 0.32	1.50 ± 0.1

water does not reach the bulk water limit, the parameter τ_0 is independent of h.

The Q dependence of the elastic and quasi-elastic intensities has been investigated by obtaining complementary information about the dynamics of hydration water.

Fig. 7 shows the relative intensity of the two Lorentzians as a function of Q, and the best fit to the spherical Bessel functions $j_0(Q)^2$ and $j_1(Q)^2$, for the case of $h = 0.3$. The $j_1(Q)$ intensity corresponds to the rotational motion and the $j_0(Q)$ intensity results from the translational motion. The resulting geometrical parameters are consistent with the analysis of the dry peptide; the radius of the sphere a_{rot}, where the rotation occurs, varies from 0.7 to 1 Å, when h increases. The x fraction of water molecules contribution, to the total scattering, changes from 0.7 to 1.

By increasing the hydration level, the elastic contribution due to water approaches zero, and the quasi-elastic contribution becomes dominant.

From the experimental elastic intensity, using the same procedure described on the previous section, we have extracted the EISF. The contribution of the first hydration water has not been taken into account, because it is completely dominated by the scattering of the new molecules. Fig. 8 represents the hydration water EISF variation as

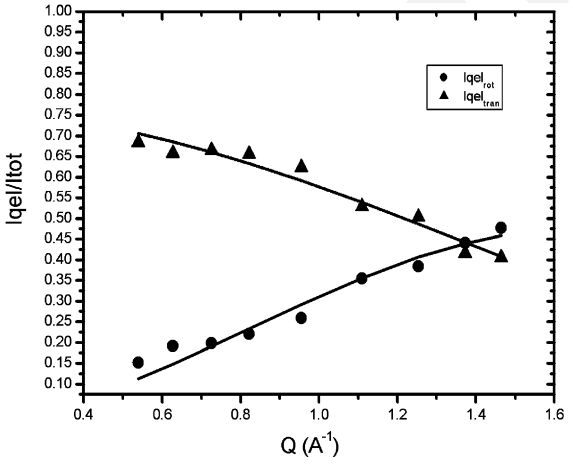

Fig. 7. Relative intensities of the two Lorentzian functions, plotted versus Q, for the hydration level $h = 0.3$. The solid line is the fit based on the $j_1(Q)$ and $j_2(Q)$ Bessel functions.

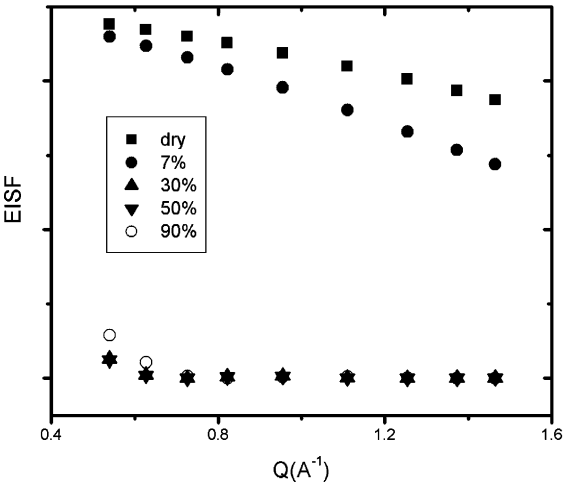

Fig. 8. EISF of hydration water plotted versus Q^2, at different hydration levels.

a function of the hydration level. The EISF hydration dependence shows a clear evolution of the dynamics between the low and high hydration levels. The EISF determined for 30%, 50% and 90% could be considered equivalent within the error bar.

A tentative of EISF analysis has been done, assuming that $\mathrm{EISF} = \mathrm{EISF}_{rot} * \mathrm{EISF}_{diff}$. EISF_{rot} has been calculated using the Bessel function of order zero, $j_0(Qa_{rot})$, with the a_{rot}, values inferred from the quasi-elastic intensity fit. The EISF_{diff} has been modeled by a simple sphere diffusion model. For all hydration levels the a_{diff} value has an average value of 5.5 A.

4. Discussion

Comparing the present results of the dynamics of hydration water of a completely hydrophobic system to those obtained for the hydration water of a completely hydrophilic system [28,29], a biological molecule [11,12] or bulk water [26], it possible to underline what is specific to our study.

Structural water present in the non-hydrated sample is characterized by a rotational motion which appears slower than that observed in bulk water at room temperature. Comparing the observed value of the characteristic rotational time

(2.2 ps) with the corresponding value for bulk water, which shows an Arrhenius behavior [26], we conclude that the dynamics of structural water is comparable to that of bulk supercooled water [28]. The value of the characteristic rotational time corresponds to a temperature which can be evaluated from the Arrhenius temperature dependence, equal to −28 °C. This can be easily understood if it is assumed that this characteristic *slow* time arises from the rotational motion of the hydrogen atom of a molecule strongly bonded to the peptide. The same trend of shifting toward lower temperatures is also observed for the dynamics of water confined in Vycor [29]. At 25% of hydration, the Vycor has one layer of hydration water [29]. Comparing the hydrogen bond life time of the confined water, at room temperature, to that one of the penta-alanine structural water, it looks slightly shorter.

Considering the case of $h = 0.07$ (three molecules of water per peptide), and assuming, from the previously presented results, that the rotational time is quite similar or even slower than that one of bulk water at the temperature of 2 °C, it appears that the dynamics of water confined in Vycor is always slightly shorter.

It is possible to generalize, stating that, in first approximation, the rotational relaxation time, of water confined in the internal hydration layer, increases in the following order: bulk water, hydrophilic site, hydrophobic site.

The values of the characteristic rotational time of the hydration water of the fully deuterated penta-alanine peptide, at the highest hydration, are identical to those found in bulk water at room temperature or in 52% hydrated Vycor. This is expected if one takes into account that there are three shells of hydration water in 52% hydrated Vycor, while for the penta peptide at hydration levels larger than 0.30 (corresponding to 9.3 molecules of water per peptide) it is plausible to consider at least two layers of water.

The same considerations apply as well for the comparison between the obtained values of the residence time in the present study and previous published work.

The most interesting case is the dynamics of the peptide hydrate at 7%. The observed residence time corresponds to that of bulk water at 2 °C. In addition, the width of the Lorentzian fits very well with that observed for bulk water at 2 °C. As presented in the previous section, the presence of diffusive motions superimposed on the rotation of the first hydrogen, generates a coupled dynamics that, in first approximation, can been described by a random rotational jump model, excluding any local diffusion.

It is worth noting that, at high hydration levels, the residence time is almost independent of hydration, in contrast with what is observed in C-phycocyanin [11,12]. This aspect could be explained by the complete homogeneity of the sample and eventually also by the lack of structural cavities which are present in a protein. However, like for the hydrated protein, in Vycor, which is also a homogeneous system, the residence time depends on the level of hydration. This is not necessarily in contradiction with our previous hypothesis. Actually the determinant factor can come from the different structure of water around hydrophilic or hydrophobic sites.

5. Conclusion

The dynamics of water as a function of its location in the vicinity of a small completely hydrophobic oligo-peptide has been studied by incoherent quasi-elastic neutron scattering. The dynamical behavior of the first interacting molecule of water has been for the first time well characterized. The results strongly suggest a characteristic slow rotational motion with a relaxation time, τ_1 of 2.2 ps, similar to what is found in supercooled water dynamics and in hydrated hydrophilic systems under supercooled conditions. Increasing the number of molecules of hydration water up to three, a coupled dynamics is observed. An experiment at different resolution could be interesting to obtain more dynamical details on this difficult case. In first approximation the dynamics has a behavior similar to that of bulk water at $T = 2$ °C.

At high hydration levels, the dynamics of hydration water approaches that of bulk water. However the residence time τ_0 presents a shift to-

wards lower temperatures as compared to a completely hydrophilic system or a biological molecule.

Comparing the different dynamics of confined water near specific sites, it has been possible to infer that, in first approximation, the rotational dynamics of the internal hydration layer slows down when one goes from bulk water to a hydrophilic site and from there to a hydrophobic site.

Acknowledgements

This work was supported by the Consorzio per lo Sviluppo di Sistemi a Grande Interfase (CSGI) and by the Commisariat à L'Energie Atomique (C.E.A.). We would like to thank Dr. Jean Marc Zanotti (LLB, Saclay) and Dr. Dominique Durand (LURE, Orsay) for valuable and stimulating discussion, Dr. Annamaria Papini (University of Florence) for using the peptide synthesizer.

References

[1] R. Parthasarathy, S. Chaturvedi, K. Go, PNAS 87 (1990) 871–875.
[2] P. Luo, R. Baldwin, PNAS 96 (1999) 4930–4935.
[3] D. Svergun, S. Richard, M.H. Koch, Z. Sayers, S. Kuprin, G. Zaccai, PNAS 95 (1998) 2267–2272.
[4] M. Ide, Y. Maeda, H. Kitano, J. Phys. Chem. B 101 (1997) 7022–7026.
[5] Y. Tamai, H. Tanaka, K. Nakanishi, Macromolecules 29 (1996) 6750.
[6] A. Kitao, F. Hirata, M. Go, J. Phys. Chem. 97 (1993) 10223.
[7] D. Hechte, F. Tadesse, L. Walters, J. Am. chem. Soc. 115 (1993) 3336.
[8] C. Andreani, A. Filabozzi, F. Menzinger, A. Desideri, A. Deriu, D. Di Cola, Biophys. J. 68 (1995) 2519–2523.
[9] M. Ferrand, A.J. Dianoux, W. Petry, G. Zaccai, PNAS 90 (1993) 9668–9672.
[10] K. Dill, Biochemistry 29 (1991) 7133.
[11] M.C. Bellissent-Funel, J. Teixeira, K.F. Bradley, S.H. Chen, J. Phys. I (France) 2 (1992) 995–1001.
[12] M.C. Bellissent-Funel, J. Teixeira, K.F. Bradley, S.H. Chen, H.L. Crespi, Physica B 180–181 (1992) 740–744.
[13] M. Tarek, D. Tobias, Biophys. J. 79 (2000) 3244–3257.
[14] S. Dellerue, M.C. Bellissent-Funel, J. Chem. Phys. 258 (2000) 315–325.
[15] J.M. Zanotti, M.C. Bellissent-Funel, J. Parello, Biophys. J. 76 (1999) 2390–2411.
[16] J.R.E. Fitter, G. Lechner, G. Buldt, N.A. Dencher, PNAS 93 (1996) 7600–7605.
[17] V. Crupi, D. Majolino, P. Migliardo, U. Wanderling, J. Macr. Struct. 480–481 (1999) 141–145.
[18] E.J. Speak, C. Olson, Z. Shi, N.R. Kallenbach, J. Am. Chem. Soc. 121 (1999) 5571–5572.
[19] A. Vila, D. Ripoli, H.A. Sheraga, PNAS 97 (no 24) (2000) 13075–13079.
[20] C.A. Rohl, A. Chakrabartty, R.L. Baldwin, Protein Sci. 5 (1996) 2623.
[21] C.A. Rhol, W. Fiori, R.L. Baldwin, PNAS 96 (1999) 3682–3687.
[22] J.K. Myer, C.N. Pace, J.M. Scholtz, Biochemistry 36 (1997) 10923.
[23] Lee et al., J. Phys. Chem. B 103 (1999) 271–275.
[24] D. Russo, J. Perez, J.M. Zanotti, D. Durand, Biophys. J. 83 (2002) 2792–2800.
[25] F. Volino, A.J. Dianoux, J. Mol. Phys. 41 (1980) 271.
[26] J. Teixeira, M.C. Bellissent-Funel, S.H. Chen, J.A. Dianoux, Phys. Rev. A 31 (1985) 1913.
[27] M.C. Bellissent-Funel, J. Teixeira, J. Mol. Struct. 250 (1991) 213–230.
[28] J. Teixeira, J.M. Zanotti, M.C. Bellissent-Funel, S.H. Chen, Physica B (1997) 234–236, also 370–374.
[29] M.C. Bellissent-Funel, S.H. Chen, J.M. Zanotti, Phys. Rev. E 51 (5) (1995) 4558–4569.